JOURNAL OF AIRCRAFT
Vol. 31, No. 4, July–Aug. 1994

Tailoring Stall Characteristics Using Leading-Edge Droop Modifications

Holly M. Ross*
NASA Langley Research Center, Hampton, Virginia 23681
and
John N. Perkins†
North Carolina State University, Raleigh, North Carolina 27695

Wind-tunnel tests were performed on a $\frac{1}{8}$-scale model of a general aviation trainer configuration in the NASA Langley 12-Foot Low-Speed Tunnel. The purpose of these tests was to investigate the configuration's high-angle-of-attack characteristics as well as the low-speed stability and control characteristics. The focus of the high-angle-of-attack testing was to develop leading-edge modifications that would tailor the stall characteristics of the model. The testing resulted in two different leading-edge modifications. A small profile leading-edge droop on the outboard 29% of the wing was developed that kept the outboard wing flow attached to high angles of attack, resulting in increased roll damping and added aileron authority. The second leading-edge modification developed was a large profile leading-edge droop on the outboard 50% of the wing. This large droop kept the outboard wing flow attached to very high angles of attack that greatly improved the roll damping characteristics and stall/departure resistance as well as provided large increases in aileron authority.

Nomenclature

b = wing span, ft
C_L = lift coefficient, lift/$q_\infty S$
C_l = rolling moment coefficient, rolling moment/$q_\infty Sb$
C_{l_β} = lateral stability derivative, $\delta C_l/\delta\beta$
C_m = pitching moment coefficient, pitching moment/$q_\infty S\bar{c}$
C_n = yawing moment coefficient, yawing moment/$q_\infty Sb$
C_{n_β} = directional stability derivative, $\delta C_n/\delta\beta$
c = local wing chord, ft
$\bar{c}$ = mean aerodynamic chord, ft
i = horizontal tail incidence, deg
q_∞ = freestream dynamic pressure, lb/ft^2
S = wing reference area, ft^2
V_∞ = freestream velocity
α = angle of attack, deg
β = angle of sideslip, deg
ΔC_l = incremental rolling moment coefficient, $C_{l_{\text{deflected}}} - C_{l_{\text{undeflected}}}$
δ_a = aileron deflection, deg
δ_e = elevator deflection, deg
δ_f = flap deflection, deg
δ_r = rudder deflection, deg

Introduction

MOST general aviation stall/spin accidents occur at low-speed flight conditions, such as takeoff and landing. In these situations the aircraft is generally at a low altitude, and thus the pilot has little time to recover control. The problem is magnified when the aircraft is a trainer with a student pilot flying. The use of wing leading-edge modifications, such as leading-edge droops, leading-edge slots, and vortex generators, has been the subject of many studies at NASA Langley Research Center. These studies have shown that these leading-edge modifications can be used successfully to improve the stall/departure characteristics of general aviation configurations and have demonstrated applications of these concepts to make several configurations spin resistant.[1–5] In many cases the leading-edge modifications that provided the large improvements did so without significantly degrading cruise performance. Improvements such as these can be achieved through comprehensive testing including low-speed wind-tunnel tests and full-scale stall and spin tests.

Leading-edge droops have primarily been used on the outboard wing to keep the flow attached to higher angles of attack and have been applied successfully on many configurations. Leading-edge droop profiles are shaped so that the maximum negative pressure peak is greatly reduced at the leading edge of the airfoil, thus decreasing or alleviating the steep adverse pressure gradient that often exists. This characteristic allows achievement of higher angles of attack without flow separation. The sharp, discontinuous edges of leading-edge droops adds to the effectiveness by creating vortical flow that energizes the local boundary layer as well as acts as an aerodynamic fence to keep the stalled inboard flow from spreading to the outboard wing, as illustrated in Fig. 1. The result of achieving more attached flow over the outboard portion of the wing is to increase roll damping at the stall and provide stall/departure resistance. Also, by keeping the outboard wing

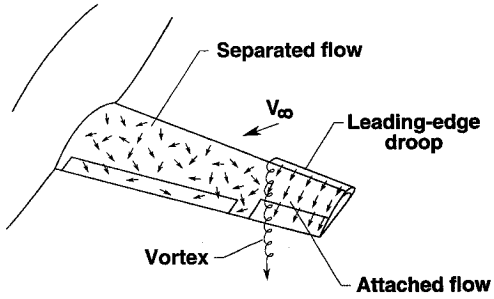

Fig. 1 Leading-edge droop aerodynamics.

Received Nov. 12, 1992; revision received April 25, 1993; accepted for publication July 21, 1993.

*Research Engineer, Flight Dynamics Branch, Flight Dynamics and Control Division, M/S 355. Member AIAA.
†Professor, Mechanical and Aerospace Engineering Department, Box 7910. Associate Fellow AIAA.

flow attached, the aileron effectiveness is generally maintained to higher angles of attack.

The configuration that was the subject of this investigation was a trainer aircraft that was designed by the Smith Aircraft Corporation. This aircraft was to have two different training roles. The first role was to provide a spinnable aircraft in which a student pilot could learn spin entry and spin recovery techniques. The second training role was to provide a spin-resistant aircraft that could be safely flown by student pilots without fear of inadvertent spins. It was thought that the two very different types of training could be accomplished with one aircraft design by modifying the wing leading edges in order to alter the high-angle-of-attack characteristics. General aviation wing designs usually incorporate some washout that improves the stall characteristics. Because the Smith design included a wing with no twist, a leading-edge modification would have to be used for both the spinnable and the spin resistant configurations to ensure good stall behavior. The leading-edge modification for the spinnable version would be used to provide a more gentle, controllable stall, while still allowing the aircraft to enter a spin. Thus, the leading-edge modification would need to be relatively small and kept on the outboard wing only. In contrast, the spin resistant configuration should have a leading-edge modification that maintains attached flow on the outboard wing to very high angles of attack in order to provide good roll damping past the stall. This would require a relatively large leading-edge droop with enough chord extension and added camber to provide the needed attached flow.

The study reported in this article investigated the high-angle-of-attack characteristics of the configurations using flow visualization, free-to-roll testing, and static force testing in a low-speed wind tunnel. These tests focused on stall characteristics and were not aimed at determining spin entry, developed spin, or spin recovery characteristics. It was the purpose of this investigation to define leading-edge modifications that could improve the stall characteristics of the spinnable configuration and greatly improve the stall/departure characteristics of the spin resistant configuration.

Description of Model and Test Techniques

A $\frac{1}{6}$-scale model of the Smith Aircraft trainer configuration was used for the wind-tunnel tests. The tests were performed at NASA Langley Research Center in the 12-Foot Low-Speed Tunnel at a freestream dynamic pressure of 4 psf which corresponded to a freestream tunnel velocity of 58 ft/s. Based on the mean aerodynamic chord, the test Reynolds number was 269,400. Data were measured over an angle-of-attack range of -5 to 40 deg, and an angle of sideslip range of -15 to 15 deg.

A three-view sketch of the model is shown in Fig. 2, and a photograph of the model mounted in the tunnel is shown in Fig. 3. A summary of the model geometric characteristics is presented in Table 1. The wing airfoil used was an NLF(1)-0414F which is designed to promote natural laminar flow. The fuselage was constructed as a fiberglass shell, and the wings

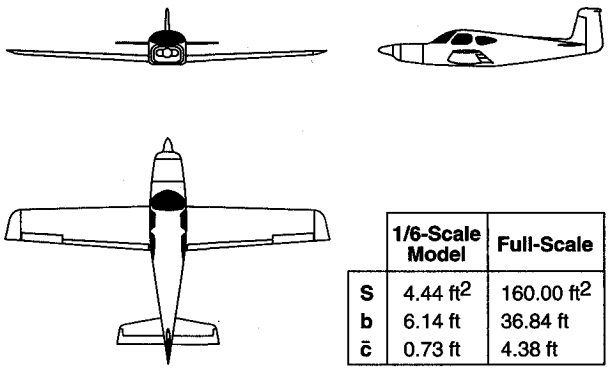

Fig. 2 Three-view sketch of model.

Table 1 Model geometric characteristics

Wing	
Area, ft²	4.44
Span, ft	6.14
Mean aerodynamic chord, ft	0.73
Root chord, ft	0.86
Tip chord, ft	0.58
Aspect ratio	8.48
Taper ratio	0.68
Wing incidence (root)	0 deg
Dihedral angle	3 deg
Twist	0 deg
Leading-edge sweep angle	1.3 deg
Trailing-edge sweep angle	3.88 deg
Airfoil	NLF(1)-0414F
Slotted flap	
Area (one), ft²	0.30
Inboard wing station	4.42
Outboard wing station	23.72
Span (per side), ft	1.61
Chord, percent c	25
Aileron	
Area (one), ft²	0.13
Inboard wing station	23.72
Outboard wing station	33.11
Span, ft	0.78
Chord, percent c	25
Horizontal tail	
Area, ft²	0.81
Span, ft	1.92
Root chord, ft	0.52
Tip chord, ft	0.35
Incidence (adjustable)	-2 to 2 deg
Elevator area, ft²	0.32
Airfoil	NACA 66-009
Vertical tail (including rudder)	
Area (reference), ft²	0.43
Span (reference), ft	0.84
Root chord (reference), ft	0.68
Tip chord, ft	0.39
Rudder area, ft²	0.26
Airfoil	NACA 66-009

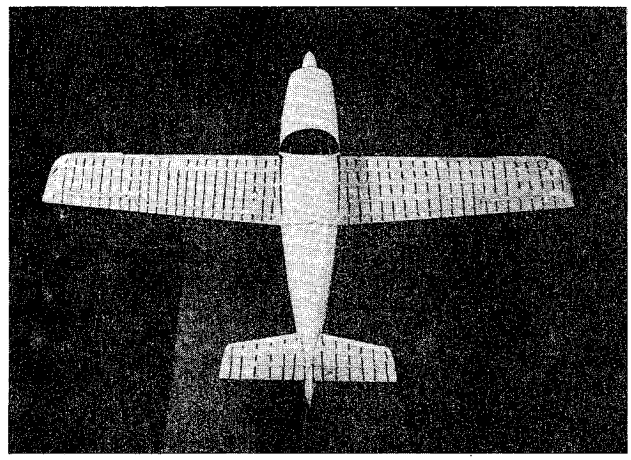

Fig. 3 Photograph of model mounted in the wind tunnel.

and tails were made of solid balsa wood. The spinner was the type used on radio-controlled models, but no propeller was installed. The model incorporated a conventional elevator, ailerons, and rudder and had slotted trailing-edge flaps. The control surface deflection ranges were as follows: $\delta_e = -20$ to $+8$ deg, $\delta_f = 0$ to $+20$ deg, $\delta_a = -20$ to $+20$ deg, and $\delta_r = -35$ to $+35$ deg, where positive values indicate trailing-

edge down or trailing-edge left deflections. Radio-controlled model-type servo-actuators were used to remotely deflect all of the control surfaces except for the flaps which were set with brackets. The horizontal stabilizer incidence was adjustable up and down by 2 deg.

Two different leading-edge droop profiles were tested and are shown in Fig. 4. Figure 4a shows the small droop, the profile selected to provide gentle stall characteristics for the spinnable configuration, and Fig. 4b shows the large droop, the profile selected to provide stall departure resistance for the spin resistant configuration. The small droop has the same leading-edge droop profile as tested on the Cessna T-210 outfitted with a natural laminar flow (NLF) wing tested in the Langley 30- by 60-Foot Tunnel.[6] This droop was designed using the leading-edge contour of an NLF(1)-0215 airfoil faired into the NLF(1)-0414 original airfoil. The derived airfoil shape was intended to keep laminar flow over the upper and lower surfaces. The large droop was designed using a two-dimensional droop design computer code which iterated on many input parameters, trying to decrease or alleviate the large negative pressure peak that occurred at the leading edge of the NLF(1)-0414F airfoil while keeping within prescribed limits on several other design values. This droop profile was not predicted to maintain laminar flow, and thus a drag penalty would be expected.

Free-to-roll tests were performed in order to determine suitable lengths for the leading-edge droops. This type of testing involves mounting the model on a special rig that allows the model to move freely about the roll axis. The free-to-roll technique was used because it gives a good indication of roll damping and stall/departure resistance. For this study, data gathered by this form of testing were purely qualitative. The runs were videotaped, and observations were made regarding the angle of attack at which wing rock occurred and the relative magnitude. A great number of runs were made this way, and a large test matrix of leading-edge droop sizes and locations could be completed quickly.

Free-to-roll testing was used to determine desired lengths of the droops. The procedure followed was to first test a droop on the outboard 50% of the wing. Then 1 in. was cut from the inboard side of the droops and the resulting configuration was tested. This procedure was followed until a trend developed relating the droop span to roll damping characteristics as determined from the wing rock displayed. From this information, the final droop spans were decided.

After the free-to-roll testing was completed, static force tests were performed to quantify the effects of the leading-edge droops on force and moment characteristics. Longitudinal and lateral-directional stability characteristics were investigated, as was the control effectiveness.

Very thin mylar tufts were used for flow visualization on the upper surface of the wing for all of the configurations tested. The tufts were used for the free-to-roll tests and the static force tests. Flow visualization results from the static force testing were used to chart the wing stall progression of the various configurations.

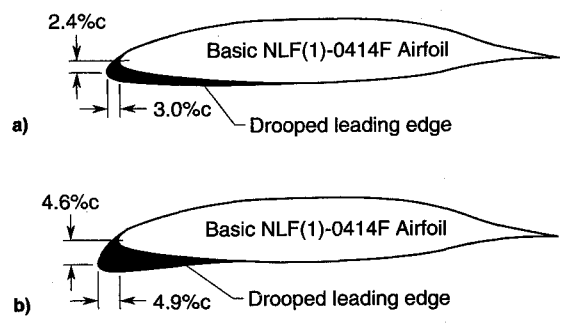

Fig. 4 Leading-edge droop modifications: a) small droop profile and b) large droop profile.

Results and Discussion

Free-to-Roll and Flow Visualization Results

Baseline Configuration

A stall map showing the stalled flow progression of the unmodified wing with the flaps undeflected was made from the tuft patterns and is shown in Fig. 5. Separation first occurred at the wing-fuselage juncture near the trailing edge of the wing at $\alpha = 8$ deg. This area of separated flow spread outboard with increased angle of attack. At $\alpha = 12$ deg, a stall cell began to form on the flap trailing edge, and by $\alpha = 14$ deg, 75% of the wing was stalled. Large amplitude roll oscillations began at $\alpha = 16$ deg, due to the loss of roll damping, and continued until $\alpha = 23$ deg, at which point the wing flow was completely separated.

Small Leading-Edge Droop Configuration

The flow visualization results for all of the small droop spans tested showed that the wing area behind the droop span maintained attached flow up to high angles of attack. Thus, the amount of attached flow could be increased by simply increasing the droop span. The free-to-roll tests performed with $\delta_f = 0$ deg showed that a droop on the outboard 50% of the wing provided enough roll damping to prevent wing rock. It was shown that a shortened droop span maintained less attached flow, but still demonstrated good roll damping characteristics. The smallest droop span tested was 7 in. (inboard edge located at 29% $b/2$). This droop length kept attached flow over the ailerons and over the outboard section of the wing. It also provided enough roll damping to prevent all but a slight wing drop at $\alpha = 16$ deg. Because the results were so predictable with changing droop span, an optimized span could easily be determined in flight tests. It was believed that this droop would not inhibit a spin entry; however, free-to-roll testing could not provide such information. Free-to-roll tests were also performed with flap deflections of 10 and 20 deg, which showed only slight degradations in the roll damping characteristics.

Figure 6 shows the stall map for the 7-in. small droop configuration. As expected, the inboard section of the wing was generally unaffected by the outboard droop. Up to $\alpha = 20$ deg, the flow directly behind the droop remained attached, whereas the unmodified wing flow was completely separated except on the wingtip. This improvement in the outboard flow provided the increased roll damping observed in the free-to-roll testing. Figure 6 also shows that the ailerons had attached flow up to $\alpha = 18$ or 20 deg, which improved the lateral control capability at high angles of attack.

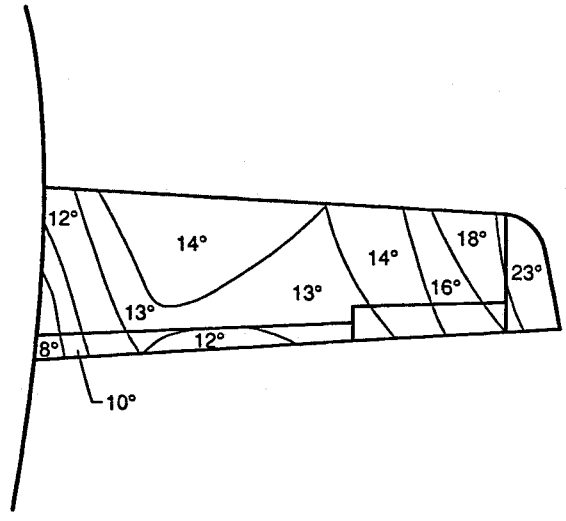

Fig. 5 Unmodified wing stall pattern. Numbers indicate the angle of attack at which separated flow first occurred.

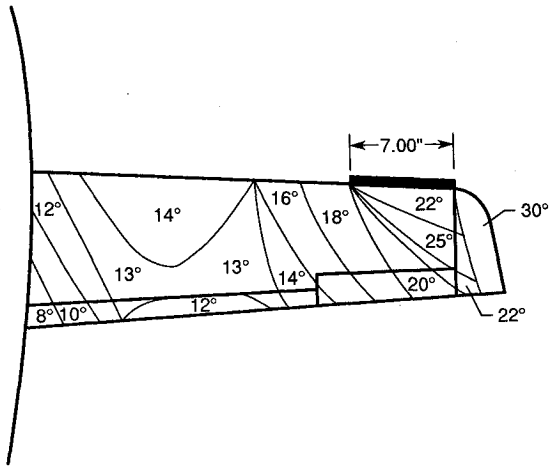

Fig. 6 Small droop configuration stall pattern.

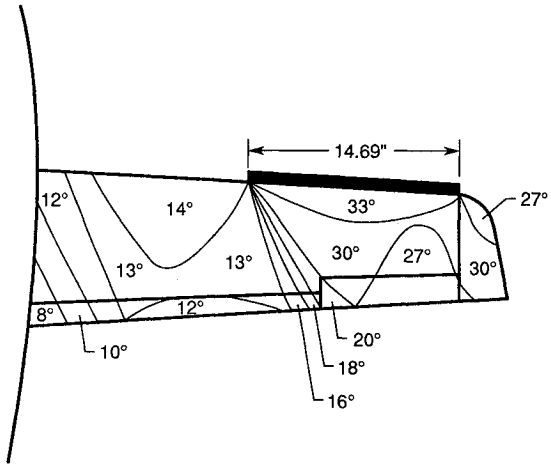

Fig. 7 Large droop configuration stall pattern.

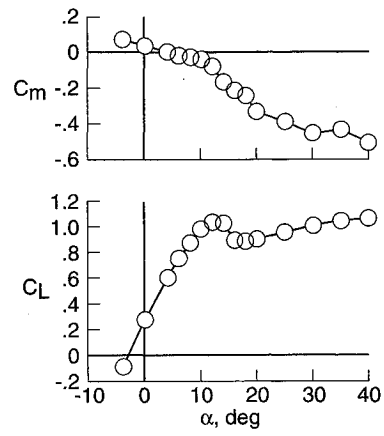

Fig. 8 Longitudinal characteristics, unmodified configuration.

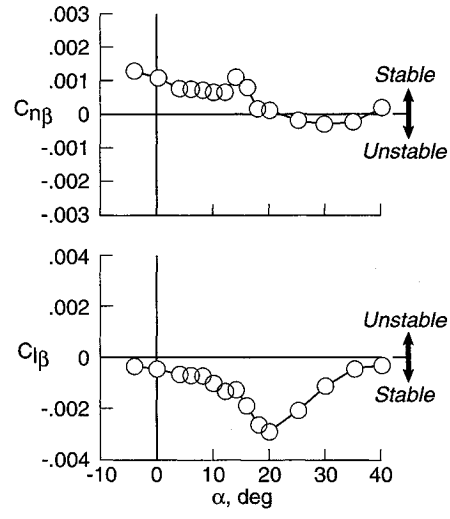

Fig. 9 Lateral-directional stability characteristics, unmodified configuration.

Large Leading-Edge Droop Configuration

The large leading-edge droop results were similar to those for the small droop. The large droop promoted attached flow on the wing directly behind the droop span up to high angles of attack, and therefore, increased the roll damping. The span determined to be the best was 14.69 in. (inboard edge located at 50% $b/2$) for $\delta_f = 0$ deg. At this span, the droop provided attached flow over nearly half of the wing up to $\alpha = 27$ deg, as shown in Fig. 7, and provided enough roll damping to prevent wing rock for all the angles of attack tested. The ailerons had attached flow until $\alpha = 27$ deg, indicating good aileron control. Free-to-roll tests performed with $\delta_f = 10$ and 20 deg demonstrated only slight degradations in the roll damping characteristics. The large droop configuration was deemed stall departure resistant and possibly spin resistant; however, spin resistance could not be determined by the tests conducted in this study.

Static Force Test Results

Baseline Configuration

Presented in Fig. 8 are the lift and pitching moment characteristics of the baseline configuration. The lift curve shows that the maximum lift occurred between $\alpha = 12$ and 14 deg. The lift curve dropped sharply after that point, indicating an abrupt stall. The pitching moment data, reduced using a c.g. location of 25% $\bar{c}$, showed good longitudinal stability at low angles of attack. The stability was reduced somewhat at $\alpha = 6$ deg, but the stability was improved after the stall. Flow visualization showed that the increased pitchdown that occurred after $\alpha = 12$ deg was due to the separation of flow on the wing while the attached flow was maintained on the horizontal tail.

The lateral-directional stability characteristics of the baseline configuration are presented in Fig. 9. The derivatives C_{n_β} and C_{l_β} were obtained from tests conducted at sideslip angles of 5 and -5 deg. The directional stability, as shown in the C_{n_β} vs α plot, was good at low angles of attack, but at $\alpha = 18$ deg, the directional stability approached neutral and became unstable at $\alpha = 22$ deg. This was due to the vertical tail becoming immersed in the stalled wake of the wing at these higher angles of attack, and thus losing its effectiveness. The lateral stability, as shown in the C_{l_β} vs α plot, shows negative values of C_{l_β} for the entire angle-of-attack range tested, indicating stable effective dihedral.

Small Leading-Edge Droop Configuration

The lift and pitching moment characteristics which compare the small droop profile with a 7-in. span to the unmodified wing are shown in Fig. 10. The unmodified wing data shown in Fig. 10 were taken with a horizontal tail incidence of $i = 0$ deg. The tail incidence was later changed to $i = 1$ deg, trailing edge up, in order to better represent the design trim specifications. The data shown for the small droop configuration was taken with $i = 1$ deg. Comparison of lift curves for the two configurations show that the small droop configuration closely resembled the unmodified wing at low angles of attack, but had a slightly higher value of $C_{L\text{-max}}$. Most notable was the effect of the small droop above $C_{L\text{-max}}$. The small droop configuration showed an increment in lift which made

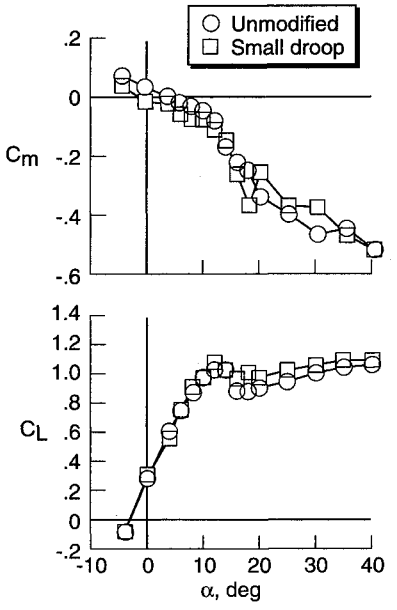

Fig. 10 Longitudinal characteristics, small droop configuration.

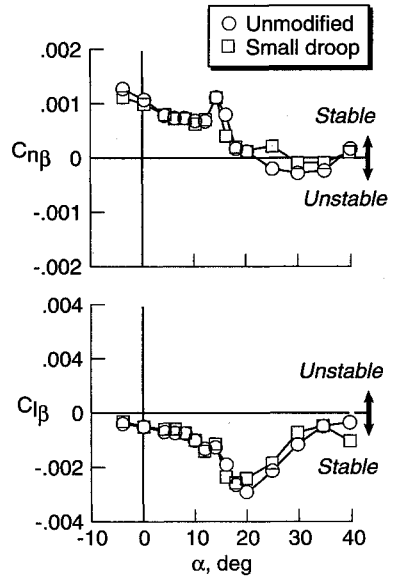

Fig. 11 Lateral-directional stability characteristics, small droop configuration.

the stall more gradual. The added lift came from the attached flow that the droop provided at angles of attack where the unmodified wing had separated flow. Thus, the small droop improved the stall characteristics. The longitudinal stability of the small droop configuration decreased between $\alpha = 8$ and 10 deg, but broke stable after the stall. The pitching moment trim change was due to the difference in tail incidences as previously discussed.

Figure 11 shows the lateral-directional characteristics of the small droop configuration compared to the unmodified wing. The directional stability is essentially unchanged with the small droop for the low angles of attack, but a slight improvement occurred between $\alpha = 20$ and 28 deg. In this region, the unmodified configuration was unstable, but the small droop configuration was stable. The lateral stability showed only negligible changes due to the modification.

Figure 12 shows a comparison of maximum aileron effectiveness for the unmodified wing and the small droop configuration. The control power for low angles of attack differed insignificantly for the two configurations. However, at $\alpha = 10$ deg, the unmodified wing started to lose aileron authority abruptly, while the small droop configuration was able to

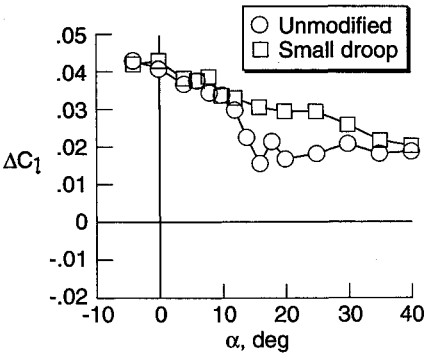

Fig. 12 Effect of the small droop modification on the maximum lateral control authority.

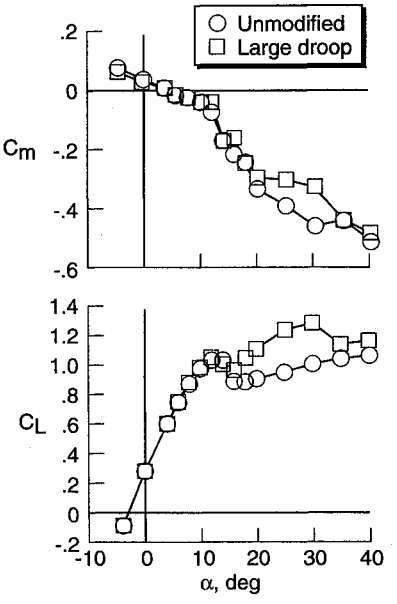

Fig. 13 Longitudinal characteristics, large droop configuration.

maintain good authority until about $\alpha = 25$ deg. This was due to the attached flow on the outboard wing that the small droop modification provided. The additional lateral control gained at the stall and beyond would improve the pilot's ability to counteract any roll-off that might occur at high angles of attack.

Large Leading-Edge Droop Configuration

The lift and pitching moment characteristics for the large leading-edge droop modification are presented in Fig. 13. The lift curve showed no major changes compared to the unmodified wing at low angles of attack, and only a slight increase in the stall C_L. As with the small droop, the real benefit of the large droop was the increment in lift above stall that resulted in a more gradual stall. The lift curve reflects the stall pattern seen in the tuft flow visualization (Fig. 7). After the initial separation that occurred on the inboard wing, the outboard wing flow remained attached until between $\alpha = 27$ and 33 deg, which is reflected in the additional lift at these high angles of attack. The longitudinal stability for the large droop configuration decreased before stall and was neutrally stable between $\alpha = 10$ and 12 deg. Similar behavior was also seen for the small droop configuration.

Presented in Fig. 14 are the lateral-directional stability characteristics for the large droop configuration. The directional stability was degraded from the unmodified wing configuration after $\alpha = 12$ deg, and became unstable at $\alpha = 18$ deg. Because this configuration was designed to be spin resistant, directional instability would be an undesirable characteristic. Although it was not pursued in this study, the addition of a ventral fin or added vertical tail area could improve this sit-

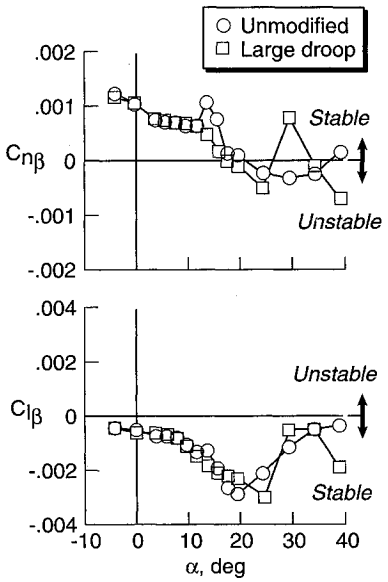

Fig. 14 Lateral-directional stability characteristics, large droop configuration.

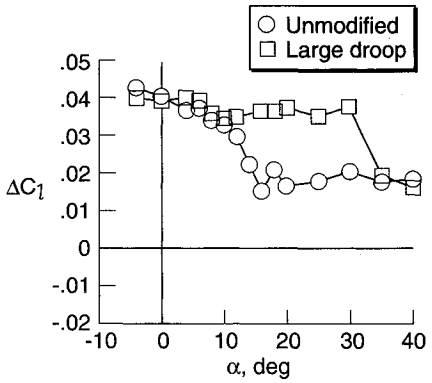

Fig. 15 Effect of the large droop modification on the maximum lateral control authority.

uation. The spike in the data that occurred at $\alpha = 30$ deg is believed to be due to an asymmetric separation of flow behind the droop at that angle of attack. Only insignificant changes were seen in lateral stability compared to the unmodified configuration.

The effect of the large droop on the maximum lateral control authority is shown in Fig. 15. These data show that the large droop maintained a very high level of roll control up to $\alpha = 30$ deg, due to the attached flow on the outboard wing sections. Except for a small loss around $\alpha = 14$ deg, the aileron control authority remained nearly constant from $\alpha = 0$ to 30 deg. In the 15- $\leq \alpha \leq$ 30-deg region, the control authority was close to twice the authority of the unmodified wing. The added control gained by the droops would enable a pilot to maintain near full lateral control up to and beyond stall.

Summary of Results

A wind-tunnel investigation was performed on a general aviation trainer configuration in order to define two different leading-edge modifications that could tailor the aircraft's high-angle-of-attack characteristics. Also, static stability and control characteristics were evaluated. The major results of this test are summarized below:

1) The baseline configuration had an abrupt stall as shown by flow visualization and static force data. The free-to-roll tests showed large amplitude roll oscillations between $\alpha =$ 16 and 23 deg, due to the loss in roll damping caused by outboard wing flow separation.

2) A small, outboard leading-edge droop with a 7-in. span (inboard edge located at 29% $b/2$) was found to be effective in keeping the outboard wing flow attached to high angles of attack, making the stall less abrupt and providing an improvement in roll damping. This modified configuration showed minimal wing rock in the free-to-roll tests. Also, aileron authority was improved for angles of attack past stall due to the increase in attached flow over the ailerons.

3) A large, outboard leading-edge droop on the outboard 50% of the wing was found to be effective in keeping the outboard wing flow attached to very high angles of attack, making the stall less abrupt and greatly improving the roll damping. This modified configuration showed no wing rock in the free-to-roll tests. Also, aileron authority was maintained up to very high angles of attack due to the increase in attached flow over the ailerons.

4) The longitudinal stability of the baseline and both modified configurations were good at low angles of attack, but degraded as stall was approached. Both the small droop and large droop configurations showed a decrease in longitudinal stability near the stall, but had good stability characteristics after the stall break.

5) The lateral-directional stability characteristics of the baseline configuration were good except for the high-angle-of-attack region where the configuration became directionally unstable. The small droop configuration showed a slight increase in directional stability for high angles of attack, but showed no appreciable change in lateral stability. The large droop configuration showed degraded directional stability at high angle of attack compared to the unmodified configuration, but showed no appreciable change in lateral stability.

Acknowledgments

The authors wish to thank Joseph Stickle, Paul Stough, and David Robelen of NASA Langley Research Center, Hampton, Virginia, for their input and help on this research project; and Mike Smith and Bob Stewart of Smith Aircraft Corp., Bay St. Louis, Mississippi, for their involvement.

References

[1]Staff of Langley Research Center, "Exploratory Study of the Effects of Wing Leading-Edge Modifications on the Stall/Spin Behavior of a Light General Aviation Airplane," NASA TP-1589, Dec. 1979.

[2]Newsome, W. A., Satran, D. R., and Johnson, J. L., Jr., "Effect of Wing Leading-Edge Modifications of a Full-Scale, Low-Wing General Aviation Airplane," NASA TP-2011, June 1982.

[3]Stough, H. P., III, DiCarlo, D. J., and Stewart, E. C., "Wing Modification for Increased Spin Resistance," Society of Automotive Engineers Paper 830720, April 1983.

[4]Stough, H. P., III, DiCarlo, D. J., and Patton, J. M., Jr., "Flight Investigation of the Effects of an Outboard Wing Leading-Edge Modification on Stall/Spin Characteristics of a Low-Wing, Single-Engine, T-Tail Light Airplane," NASA TP-2691, July 1987.

[5]Ross, H. M., Yip, L. P., Perkins, J. N., Vess, R. J., and Owens, D. B., "Wing Leading-Edge Droop/Slot Modification for Stall Departure Resistance," *Journal of Aircraft*, Vol. 28, No. 27, 1991, pp. 436–442.

[6]Murri, D. G., and Jordan, F. L., Jr., "Wind Tunnel Investigation of a Full-Scale General Aviation Airplane Equipped with an Advanced Natural Laminar Flow Wing," NASA TP-2772, Nov. 1987.